DTIC FILE COPY

(4)

GL-TR-89-0186

PROGRESS OF DORIS AUTOMATIC SCALING

Walter S. Kuklinski
Kavitha Chandra
Bodo W. Reinisch

University of Lowell
Center for Atmospheric Research
450 Aiken Street
Lowell, Massachusetts 01854

AD-A223 106

January 1989

DTIC
ELECTE
JUN 13 1990
S B D

Scientific Report No. 15

Approved for public release; distribution unlimited.

GEOPHYSICS LABORATORY
AIR FORCE SYSTEMS COMMAND
UNITED STATES AIR FORCE
HANSCOM AIR FORCE BASE, MASSACHUSETTS 01731-5000

"Original contains color plates: All DTIC reproductions will be in black and white"

90 06 12 139

"This technical report has been reviewed and is approved for publication"

ANTONIO QUESADA
Contract Manager

WILLIAM K. VICKERY
Branch Chief

FOR THE COMMANDER

ROBERT A. SKRIVANEK
Division Director

This report has been reviewed by the ESD Public Affairs Office (PA) and is releasable to the National Technical Information Service (NTIS).

Qualified requestors may obtain additional copies from Defense Technical Information Center.

If your address has changed, or if you wish to be removed from the mailing list, or if the addressee is no longer employed by your organization, please notify AFGL/DAA, Hanscom AFB, MA 01731. This will assist us in maintaining current mailing list.

Do not return copies of this report unless contractual obligations or notice on a specific document requires that it be returned.

REPORT DOCUMENTATION PAGE

Form Approved OMB No. 0704-0188

1a. REPORT SECURITY CLASSIFICATION: Unclassified	1b. RESTRICTIVE MARKINGS
2a. SECURITY CLASSIFICATION AUTHORITY	3. DISTRIBUTION/AVAILABILITY OF REPORT: Approved for public release; distribution unlimited.
2b. DECLASSIFICATION/DOWNGRADING SCHEDULE	
4. PERFORMING ORGANIZATION REPORT NUMBER(S): ULRF-454/CAR	5. MONITORING ORGANIZATION REPORT NUMBER(S): GL-TR-89-0186
6a. NAME OF PERFORMING ORGANIZATION: University of Lowell; 6b. OFFICE SYMBOL (If applicable):	7a. NAME OF MONITORING ORGANIZATION: NorthWest Research Associates, Inc.
6c. ADDRESS (City, State, and ZIP Code): Center for Atmospheric Research, 450 Aiken Street, Lowell, MA 01854	7b. ADDRESS (City, State, and ZIP Code): 300 120th Avenue, NE, Bellevue, WA 98005
8a. NAME OF FUNDING/SPONSORING ORGANIZATION: Geophysics Laboratory; 8b. OFFICE SYMBOL (If applicable): LIS	9. PROCUREMENT INSTRUMENT IDENTIFICATION NUMBER: F19628-87-C-0003
8c. ADDRESS (City, State, and ZIP Code): Hanscom AFB, Massachusetts 01731-5000	10. SOURCE OF FUNDING NUMBERS: PROGRAM ELEMENT NO. 62101F; PROJECT NO. 4643; TASK NO 10; WORK UNIT ACCESSION NO. AC

11. TITLE (Include Security Classification)
Progress of DORIS Automatic Scaling

12. PERSONAL AUTHOR(S)
Walter S. Kuklinski; Kavitha Chandra; Bodo W. Reinisch

13a. TYPE OF REPORT	13b. TIME COVERED	14. DATE OF REPORT (Year, Month, Day)	15. PAGE COUNT
Scientific #15	FROM _____ TO _____	1989 January	24

16. SUPPLEMENTARY NOTATION

17. COSATI CODES		
FIELD	GROUP	SUB-GROUP

18. SUBJECT TERMS (Continue on reverse if necessary and identify by block number)
Algorithm; Oblique Ionogram; Scaling; Trace Enhancement; Frequency; Vertical Ionogram

19. ABSTRACT (Continue on reverse if necessary and identify by block number)

A major component of the Digital Oblique Remote Ionospheric Sensing program (DORIS) is the development of an automatic oblique ionogram scaling algorithm. The nature of the variations that have been observed in oblique ionograms collected to date has required the use of adaptive signal processing and pattern recognition techniques in the development of this oblique ionogram scaling algorithm. An extensive data base of digital oblique ionograms will be required to develop, test, and verify the performance of the scaling algorithm. The continuing efforts in data collection and the associated parallel effort in the development of the oblique ionogram scaling algorithm is discussed in this report. Results obtained to date have lead to a modification of the initially proposed oblique ionogram scaling algorithm. These modifications, discussed in detail in the following section, have produced a more robust as well as a more computationally efficient oblique ionogram scaling algorithm.

20. DISTRIBUTION/AVAILABILITY OF ABSTRACT	21. ABSTRACT SECURITY CLASSIFICATION
☐ UNCLASSIFIED/UNLIMITED ☐ SAME AS RPT ☐ DTIC USERS	Unclassified
22a. NAME OF RESPONSIBLE INDIVIDUAL: Antonio Quesada	22b TELEPHONE (Include Area Code)	22c. OFFICE SYMBOL: GL/LIS

DD Form 1473, JUN 86 *Previous editions are obsolete.*

TABLE OF CONTENTS

		Page
1.0	INTRODUCTION	1
2.0	REFINEMENT OF OBLIQUE IONOGRAM SCALING ALGORITHM	2
3.0	EVALUATION OF OBLIQUE TRACE ENHANCEMENT ALGORITHM	6
4.0	OBLIQUE IONOGRAM SCALING ALGORITHM STATUS	17

DTIC COPY INSPECTED 6

Accession For
NTIS GRA&I ☑
DTIC TAB ☐
Unannounced ☐
Justification
By
Distribution/
Availability Codes
Dist | Avail and/or Special
A-1

LIST OF FICURES

Figure No.		Page
2.1	Endpoint Vertical Ionogram Based Oblique Ionogram Scaling Algorithm	3
2.2	Modified Endpoint Vertical Ionogram Based Oblique Ionogram Scaling Algorithm	5
3.1	Original 25 kHz oblique ionogram (upper panel) and resulting 100 kHz ionogram produced via the frequency redundancy technique. Goose Bay, Labrador to Wallops Island, Virginia; October 27, 1988, 1201 UT.	7
3.2	Enlarged view of the 100 kHz oblique ionogram shown in Figure 2.1. Goose Bay, Labrador to Wallops Island, Virginia; October 27, 1988, 1201 UT.	7
3.3	Resulting 100 kHz oblique ionogram after processing through the modified Wiener trace enhancement algorithm and the noise suppression filter. Goose Bay, Labrador to Wallops Island, Virginia; October 17, 1988, 1201 UT.	8
3.4	Region of interest calculated from the F layer of the corresponding vertical ionogram. Synthesized oblique 1F ionogram is shown in blue. Goose Bay, Labrador to Wallops Island, Virginia; October 27, 1988, 1201 UT.	8

LIST OF FIGURES (Continued)

Figure No.		Page
3.5	Region of interest overlaid on the filtered oblique ionogram. Goose Bay, Labrador to Wallops Island, Virginia; October 27, 1988, 1201 UT.	10
3.6	Resulting oblique 1F ionogram in the region of interest. Goose Bay, Labrador to Wallops Island, Virginia; October 27, 1988, 1201 UT.	10
3.7	Scaled oblique 1F trace shown in white along with the 1F oblique ionogram. Goose Bay, Labrador to Wallops Island, Virginia; October 27, 1988, 1201 UT.	11
3.8	100 kHz oblique ionogram produced via the frequency redundancy technique. Goose Bay, Labrador to Millstone Hill, Massachusetts; April 5, 1988, 1908 UT.	11
3.9	Resulting 100 kHz oblique ionogram after processing through the modified Wienrt trace enhancement algorithm and the noise suppression filter. Goose Bay, Labrador to Millstone Hill, Massachusetts; April 5, 1988, 1908 UT.	12
3.10	Region of interest calculated from the E and F layers of the corresponding vertical ionogram. Synthesized oblique 1F (blue) and 1E (yellow) ionograms shown in the corresponding regions of interest. Goose Bay, Labrador to Millstone Hill, Massachusetts; April 5, 1988, 1908 UT.	12

LIST OF FIGURES (Continued)

Figure No.		Page
3.11	Region of interest (1F) overlaid on the filtered oblique ionogram. Goose Bay, Labrador to Millstone Hill, Massachusetts; April 5, 1988, 1908 UT.	13
3.12	Resulting oblique 1F ionogram in the region of interest. Goose Bay, Labrador to Millstone Hill, Massachusetts; April 5, 1988, 1908 UT.	13
3.13	Scaled oblique 1F trace shown in white along with the 1F oblique ionogram. Goose Bay, Labrador to Millstone Hill, Massachusetts; April 5, 1988, 1908 UT.	14
3.14	Region of interest (1E) overlaid on the filtered oblique ionogram. Goose Bay, Labrador to Millstone Hill, Massachusetts; April 5, 1988, 1908 UT.	14
3.15	Resulting oblique 1E trace shown with the region of interest. Goose Bay, Labrador to Millstone Hill, Massachusetts; April 5, 1988, 1908 UT.	15
3.16	Scaled oblique 1E trace shown in white along with the 1E oblique ionogram. Goose Bay, Labrador to Millstone Hill, Massachusetts; April 5, 1988, 1908 UT.	15

1.0 INTRODUCTION

A major component of the Digital Oblique Remote Ionospheric Sensing program (DORIS) is the development of an automatic oblique ionogram scaling algorithm. The nature of the variations that have been observed in oblique ionograms collected to date has required the use of adaptive signal processing and pattern recognition techniques in the development of this oblique ionogram scaling algorithm. An extensive data base of digital oblique ionograms will be required to develop, test, and verify the performance of the scaling algorithm. The continuing efforts in data collection and the associated parallel effort in the development of the oblique ionogram scaling algorithm is discussed in this report. Results obtained to date have lead to a modification of the initially proposed oblique ionogram scaling algorithm. These modifications, discussed in detail in the following section, have produced a more robust as well as a more computationally efficient oblique ionogram scaling algorithm.

2.0 REFINEMENT OF OBLIQUE IONOGRAM SCALING ALGORITHM

The operation of the endpoint vertical ionogram based oblique ionogram scaling algorithm presented in the Scientific Report No. 13, GL-TR-89-0184, Oblique Ionogram Automatic Scaling Algorithm - A Status Report, October 1988, can be represented by the block diagram presented in Figure 2.1. The noise suppression/ trace enhancement filter operation of this proposed algorithm was a Wiener filter that required knowledge of the power spectral densities of the residual noise/interference signal, $P_n(\omega_t,\omega_f)$, and the leading edge of the oblique ionogram, $P_n(\omega_t,\omega_f)$. In addition the two-dimensional Fourier transform of the oblique echo-trace pulse width generation filter, $H_S(\omega_t,\omega_f)$, was needed to produce the Wiener filter $H(\omega_t,\omega_f)$ given as:

$$H(\omega_t,\omega_f) = \frac{H_s^*(\omega_t,\omega_f)\, P_{1e}(\omega_t,\omega_f)}{\left|H_s(\omega_t,\omega_f)\right|^2 P_{1e}(\omega_t,\omega_f) + P_n(\omega_t,\omega_f)}$$

Examination of the behavior of this filter on oblique ionogram data for paths of 1500 and 2500 km indicated that the filter is very sensitive to $H_S(\omega_t,\omega_f)$, that represents both the oblique echo-trace pulse width and pulse shape. Since we can only approximate the oblique echo pulse shape, the oblique echo-trace pulse width generation filter, $H_S(\omega_t,\omega_f)$,.was removed from the Wiener filter, producing a modified Wiener filter $H_m(\omega_t,\omega_f)$ that produces an optimal estimate of the entire oblique echo-trace from the preprocessed oblique ionogram. $H_m(\omega_t,\omega_f)$ is:

$$H_m(\omega_t,\omega_f) = \frac{P_{1e}(\omega_t,\omega_f)}{P_{1e}(\omega_t,\omega_f) + P_n(\omega_t,\omega_f)}$$

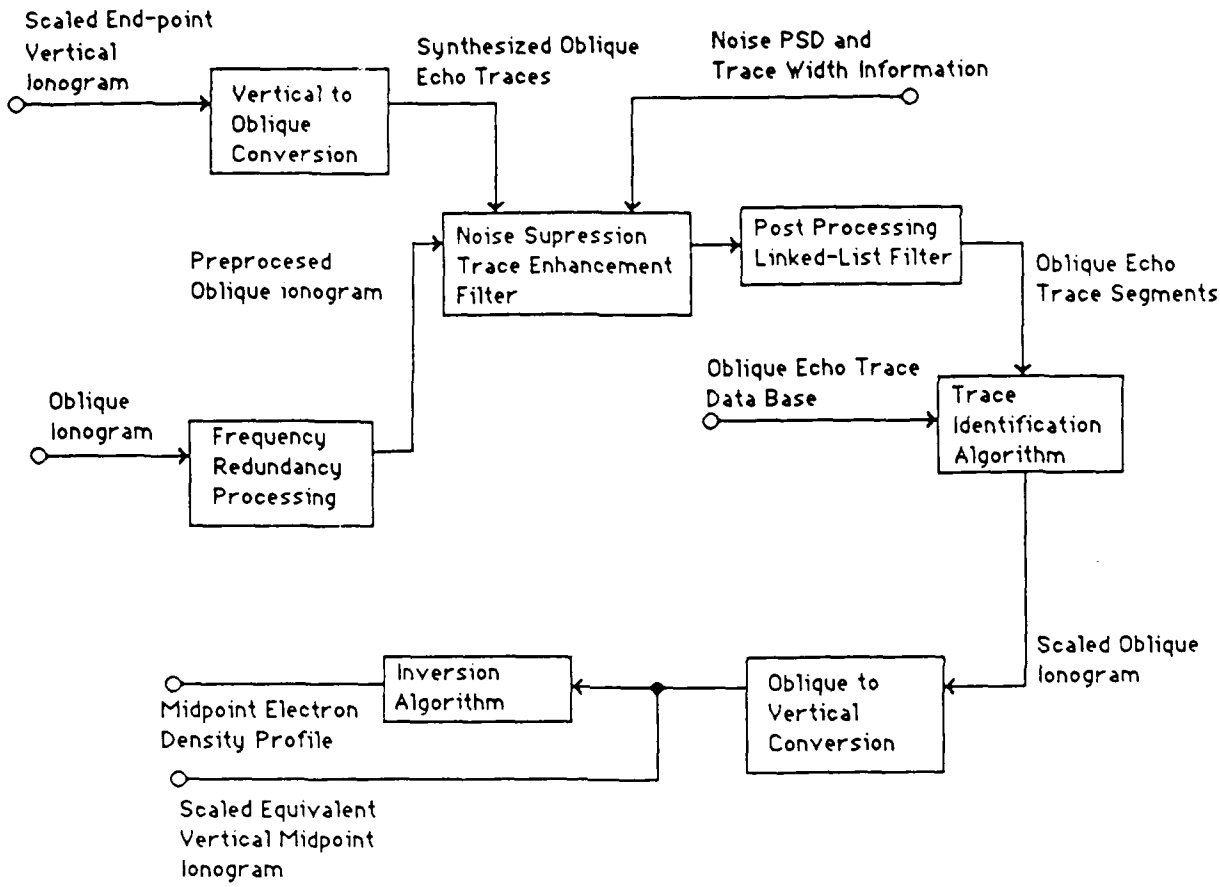

Figure 2.1 Endpoint Vertical Ionogram Based Oblique Ionogram Scaling Algorithm

With this modification, the detection of the leading edge of the oblique echo traces will take place as part of the trace identification algorithm. The modified endpoint vertical ionogram based oblique ionogram scaling algorithm can be represented by the block diagram presented in Figure 2.2.

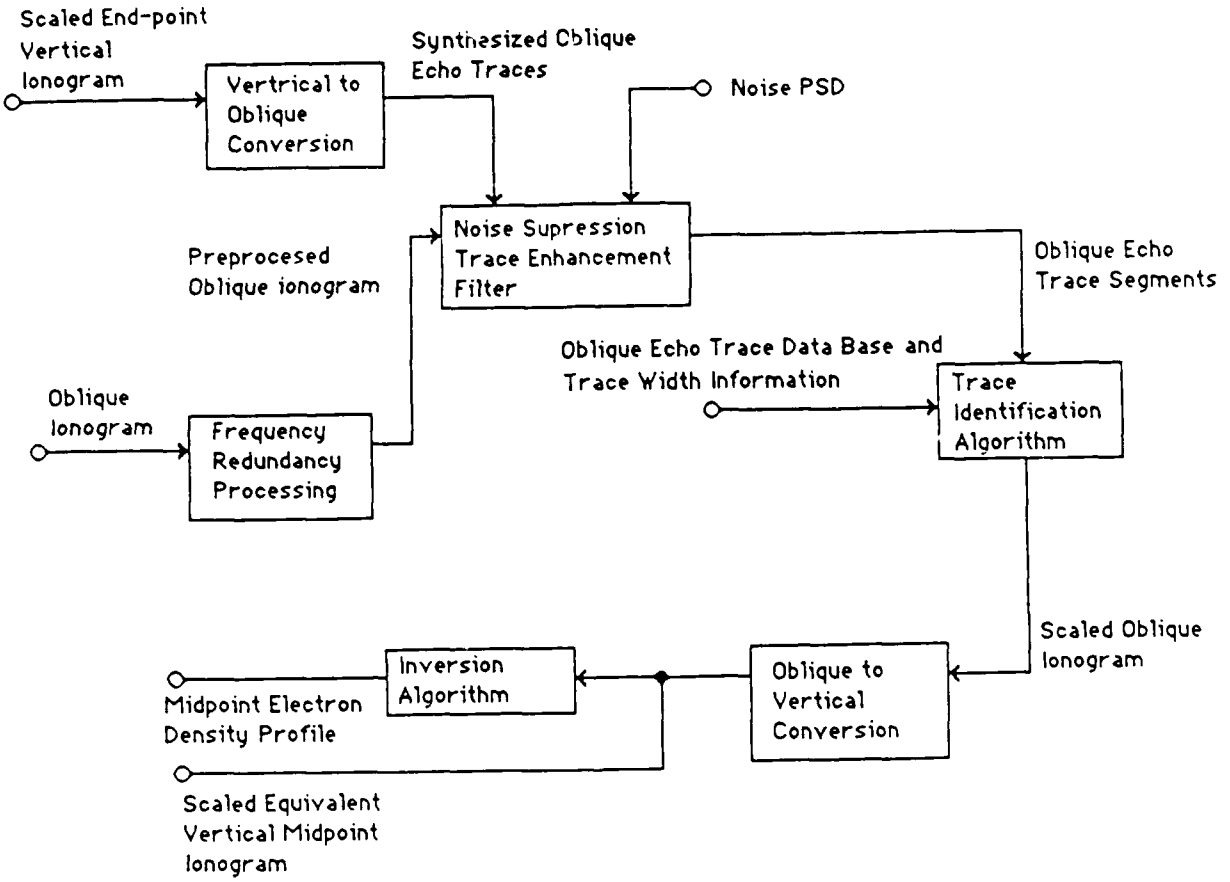

Figure 2.2 Modified Endpoint Vertical Ionogram Based Oblique Ionogram Scaling Algorithm

3.0 EVALUATION OF OBLIQUE TRACE ENHANCEMENT ALGORITHM

The performance of the modified oblique ionogram trace enhancement algorithm was evaluated using two sets of ionograms. The first data set was obtained during days 90-98 of 1988. The oblique path was approximately 1800 km long with the transmitting Digisonde 256 in Goose Bay, Canada and the corresponding receiving system at Millstone Hill Observatory in Westford, MA. The Goose Bay station used a horizontally radiating log periodic antenna, while the Millstone Hill station used the standard Digisonde seven loop antenna array. Synchronization of the two stations, which is required for oblique ionograms, was performed manually in this experiment. The vertical ionograms were produced over a frequency range of 1 to 10 MHz, using 100 kHz sounding frequency increments, while the oblique ionograms were scanned over a frequency range from 4 to 18 MHz, using 50 kHz frequency increments. The second data set was obtained during day 301 of 1988. The oblique path was approximately 2500 km long with the transmitting Digisonde 256 in Goose Bay, Canada and the corresponding receiving system at Wallops Island, VA. The vertical ionograms were also produced over a frequency range of 1 to 10 MHz, using 100 kHz sounding frequency increments, while these oblique ionograms were scanned over a frequency range from 5 to 29 MHz, using 25 kHz frequency increments.

The 2500 km oblique data is seen in Figures 3.1 - 3.7. The original 25 kHz oblique ionogram and the resulting 100 kHz ionogram, produced via the frequency redundancy technique are seen in Figure 3.1. Figure 3.2 is an enlarged view of the 100 kHz oblique ionogram. Figure 3.3. shows the resulting output of the modified Wiener trace enhancement and noise suppression filter. Figure 3.4 shows the region of interest calculated from the F layer of the corresponding vertical ionogram. The synthesized oblique F trace

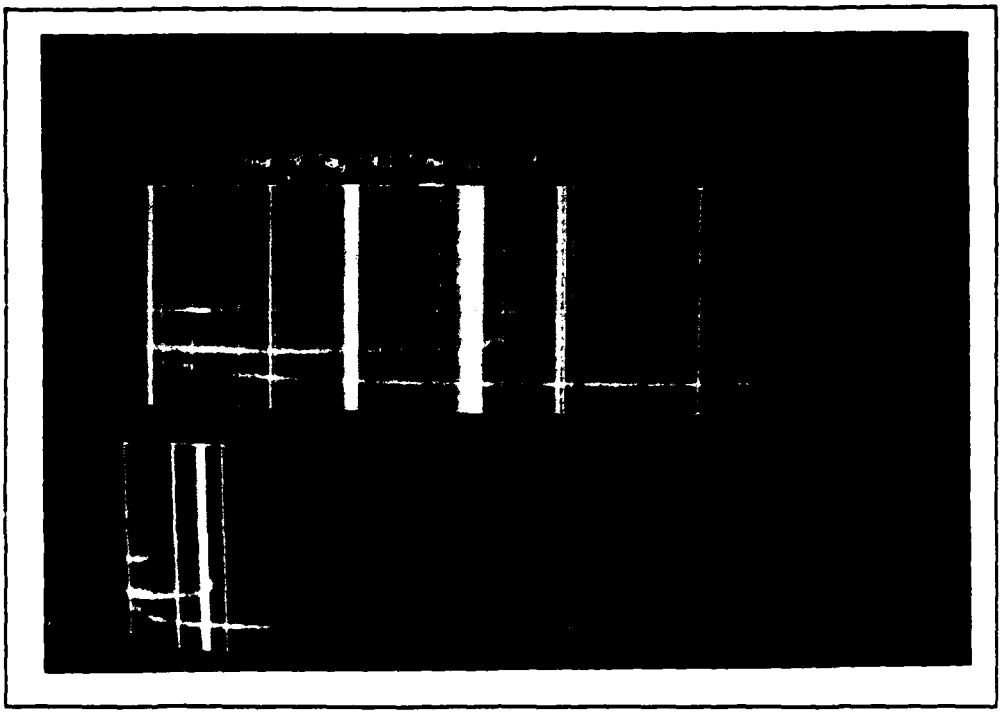

Figure 3.1 Original 25 kHz oblique ionogram (upper panel) and resulting 100 kHz ionogram produced via the frequency redundancy technique. Goose Bay, Labrador to Wallops Island, Virginia; October 27, 1988, 1201UT.

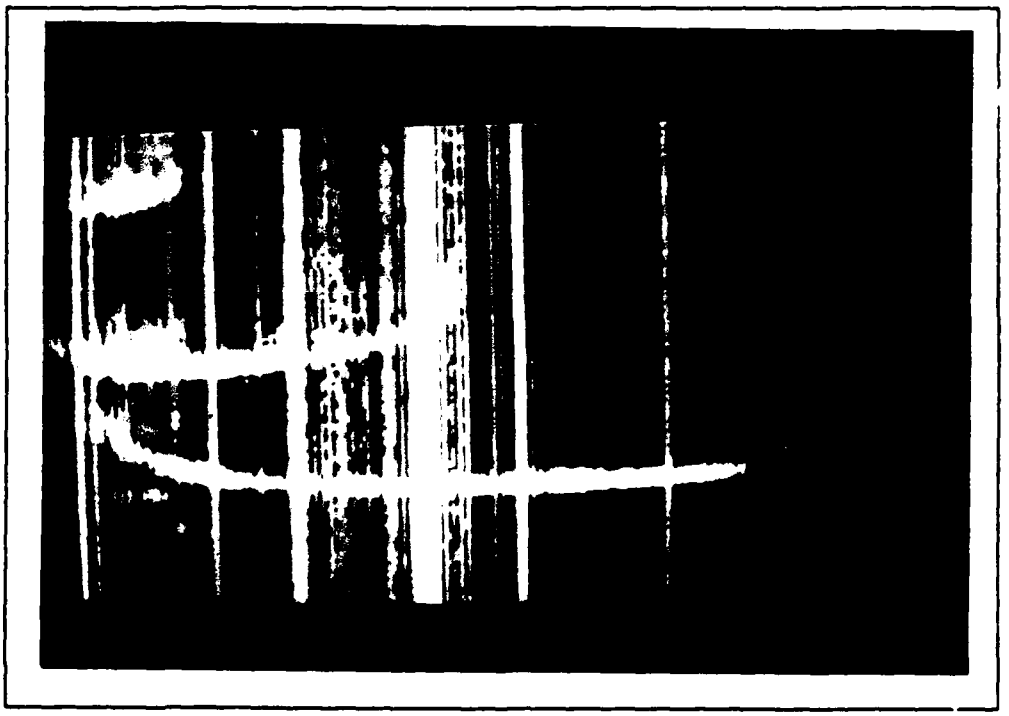

Figure 3.2 Enlarged view of the 100 kHz oblique ionogram shown in Figure 2.1. Goose Bay, Labrador to Wallops Island, Virginia; October 27, 1988, 1201UT.

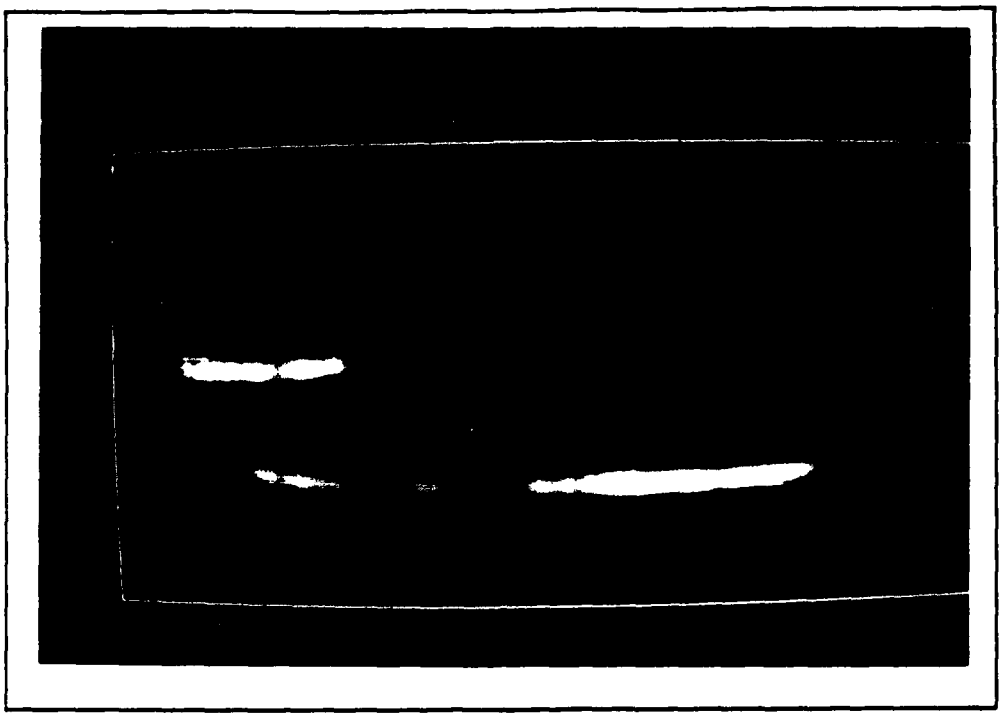

Figure 3.3 Resulting 100 kHz oblique ionogram after processing through the modified Wiener trace enhancement algorithm and the noise suppression filter. Goose Bay, Labrador to Wallops Island, Virginia; October 27, 1988; 1201UT.

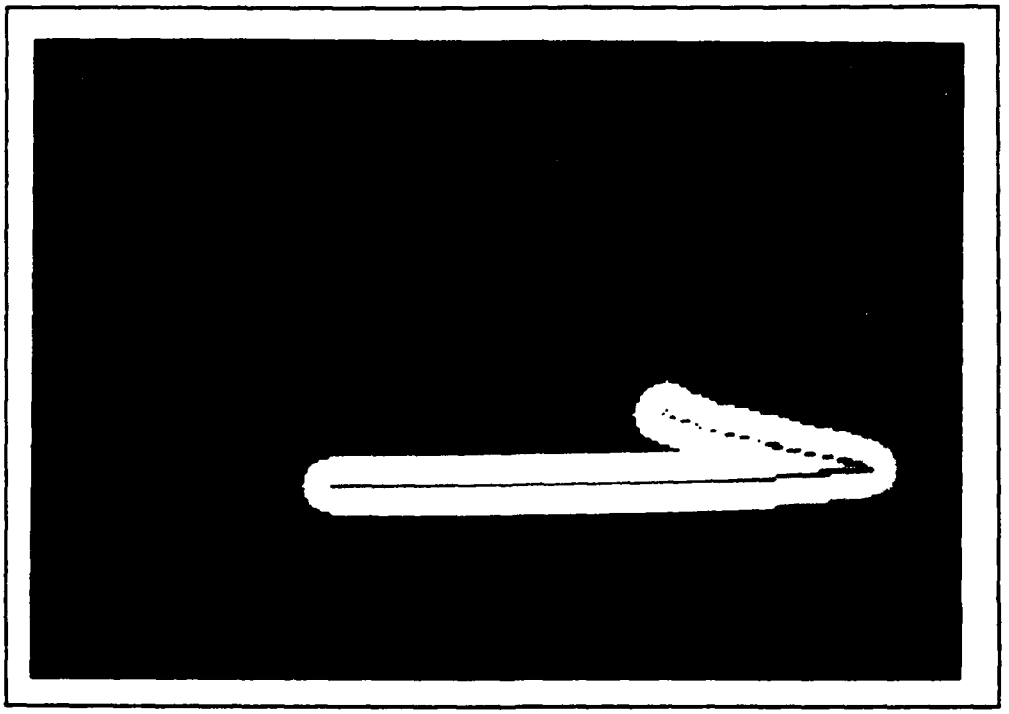

Figure 3.4 Region of interest calculated from the F layer of the corresponding vertical ionogram. Synthesized oblique 1F ionogram is shown in blue. Goose Bay, Labrador to Wallops Island, Virginia; October 27, 1988, 1201UT.

is shown in blue in the center of the white region of interest. At present the algorithm will accept any signals in this region, defined as all points within six range bins and/or sounding frequencies of the synthesized oblique F trace, as potential oblique F trace data. At a later stage of development additional information derived from an ionospheric model and information based on the total previous experience of the oblique scaling algorithm, i.e. the results of all previously scaled oblique ionograms, will be used to determine the region of interest. Figure 3.5 shows the region of interest overlaid on the filtered oblique ionogram data. Note that although all of the high angle ray portion of the one hop F oblique echo trace is within the region of interest, the actual data has a larger slope than the region of interest and hence lower frequency portions of the high angle ray, if they had been recorded, would be excluded from further processing. The retardation of the low frequency portion of the low angle ray of the F1 trace is caused by the underlying E layer. The present algorithm will be refined to include these multiple layer effects at a later time. Figure 3.6 shows the resulting oblique F echo trace, i.e. only that portion of the filtered oblique ionogram data in the region of interest. Figure 3.7 shows the resulting scaled oblique F trace in white along with the entire F oblique echo trace. In this case a simple algorithm that defined the scaled trace as the first occupied range bin following an unoccupied range bin at each sounding frequency was used.

The 1800 km oblique data is seen in Figures 3.8 - 3.16. The 100 kHz ionogram, produced via the frequency redundancy technique is seen in Figure 3.8. Figure 3.9 shows the resulting output of the modified Wiener trace enhancement and noise suppression filter. Figure 3.10 shows the regions of interest calculated from the E and F layers of the corresponding vertical ionogram. The synthesized oblique F trace is shown in blue in the center of the white region of interest with the synthesized oblique E trace shown in yellow in the center of the red region of interest. The F region of interest criteria

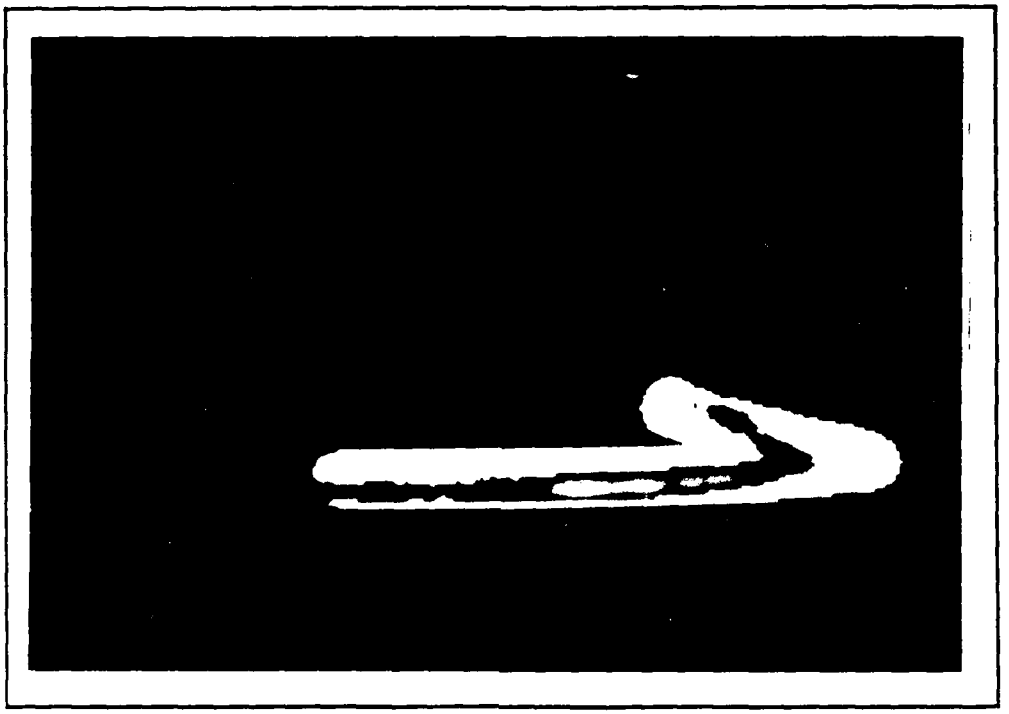

Figure 3.5 Region of interest overlayed on the filtered oblique ionogram. Goose Bay, Labrador to Wallops Island, Virginia; October 27, 1988, 1201UT.

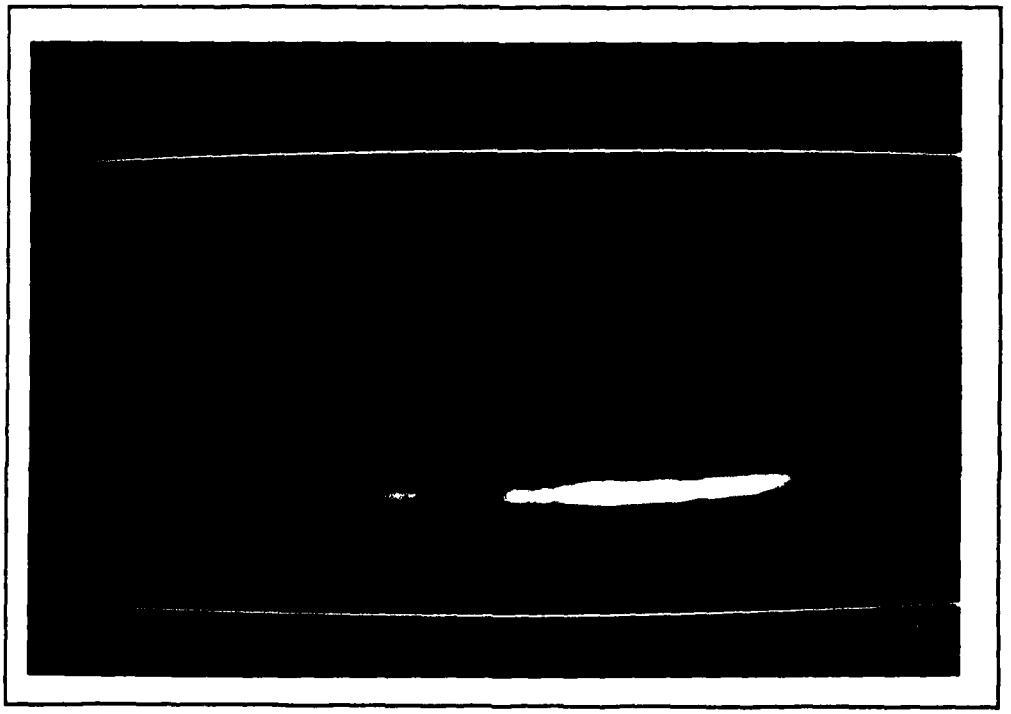

Figure 3.6 Resulting oblique 1F ionogram in the region of interest. Goose Bay, Labrador to Wallops Island, Virginia; October 27, 1988, 1201UT.

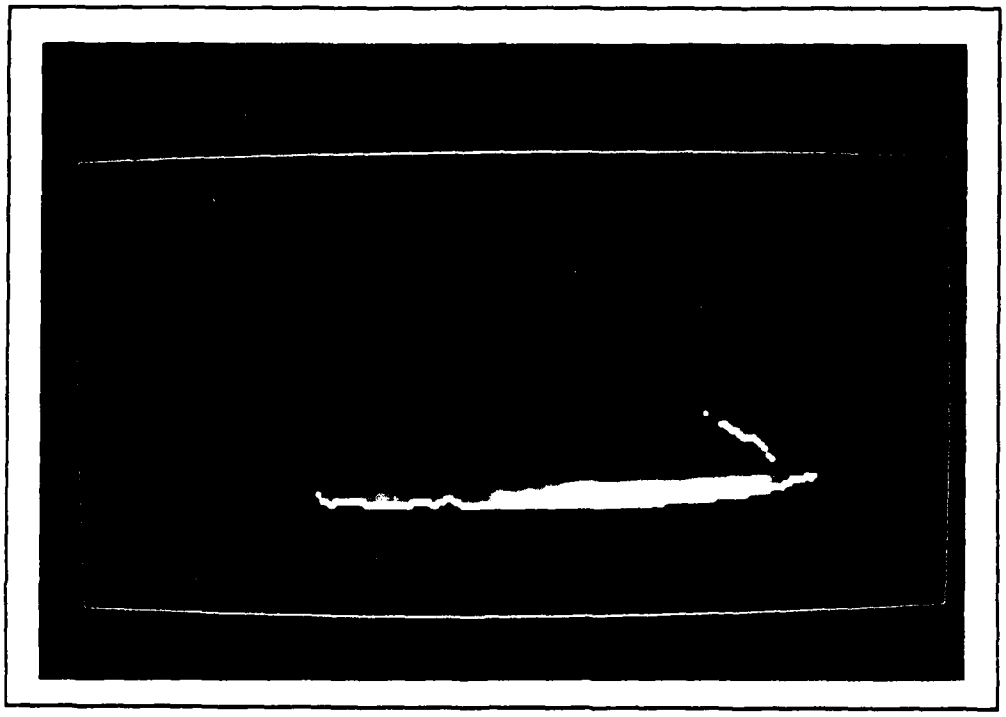

Figure 3.7 Scaled oblique 1F trace shown in white along with the 1F oblique ionogram. Goose Bay, Labrador to Wallops Island, Virginia; October 27, 1988, 1201UT.

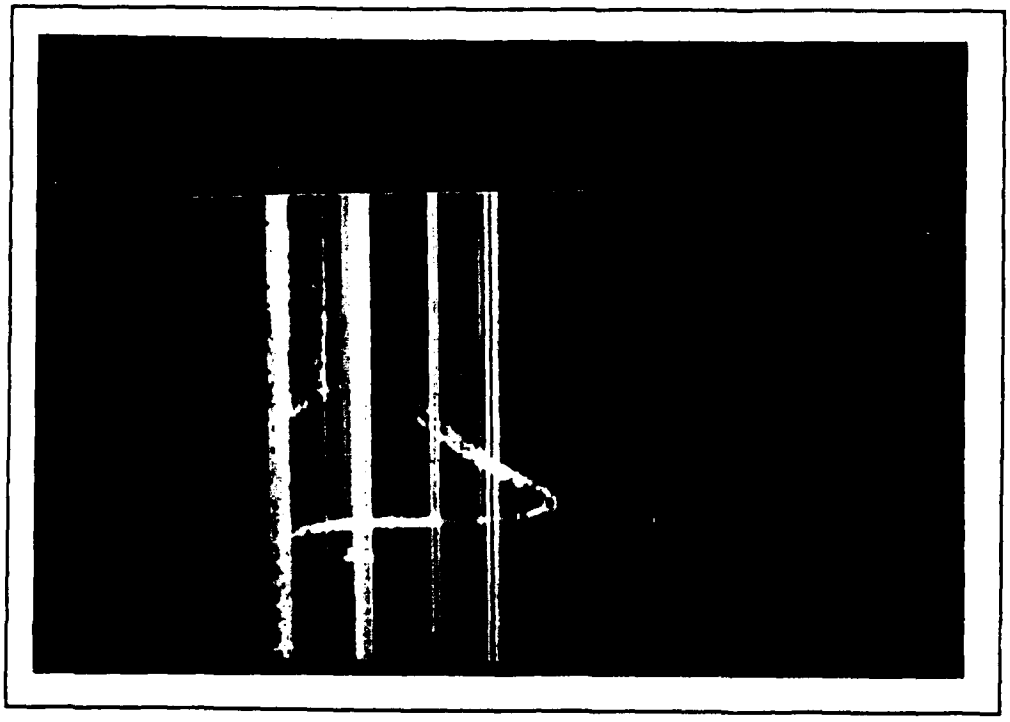

Figure 3.8 100 kHz oblique ionogram produced via the frequency redundancy technique. Goose Bay, Labrador to Millstone Hill, Massachusetts; April 5, 1988, 1908UT.

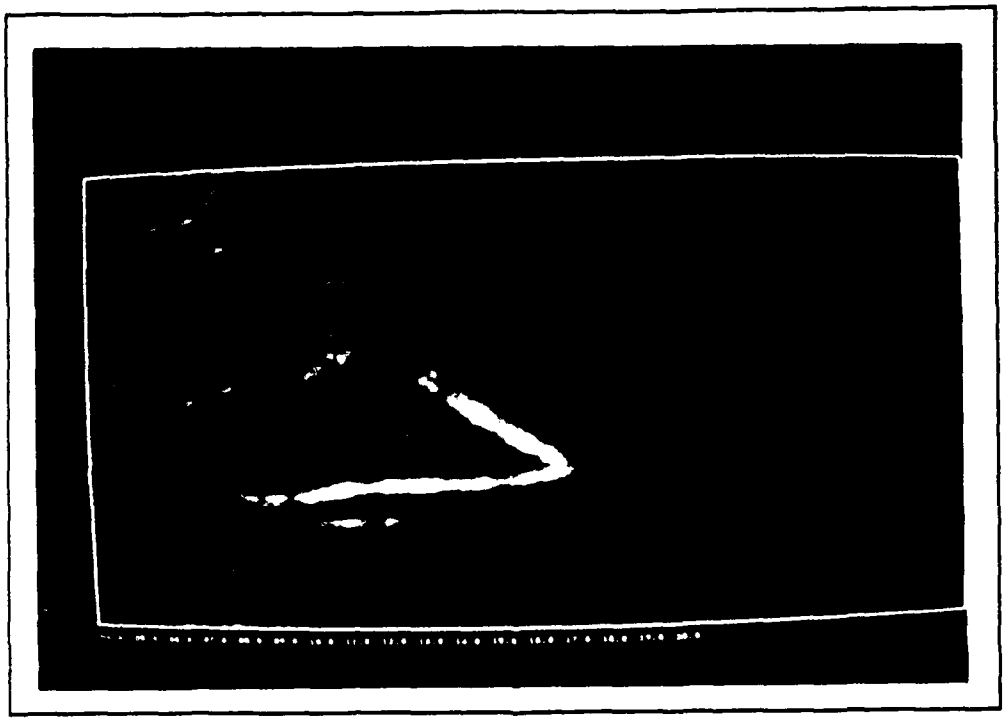

Figure 3.9 Resulting 100 kHz oblique ionogram after processing through the modified Wiener trace enhancement algorithm and the noise suppression filter. Goose Bay, Labrador to Millstone Hill, Massachusetts; April 5, 1988, 1908UT.

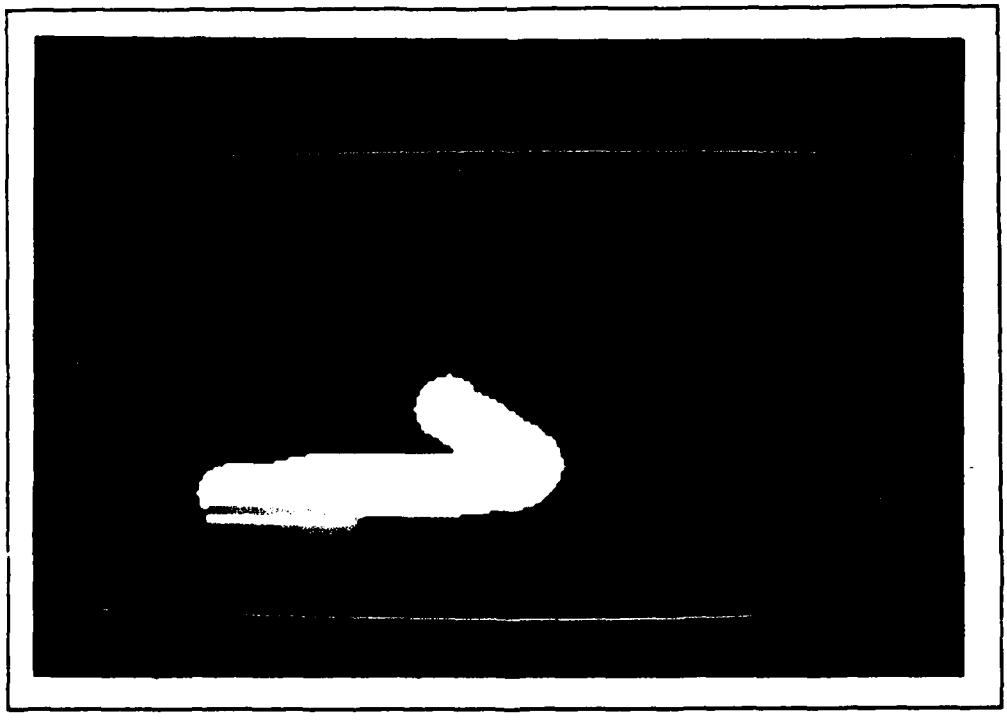

Figure 3.10 Region of interest claculated from the E and F layers of the corresponding vertical ionogram. Synthesized oblique 1F (blue) and 1E (yellow) ionograms shown in the corresponding regions of interest. Goose Bay, Labrador to Millstone Hill, Massachusetts; April 5, 1988, 1908UT.

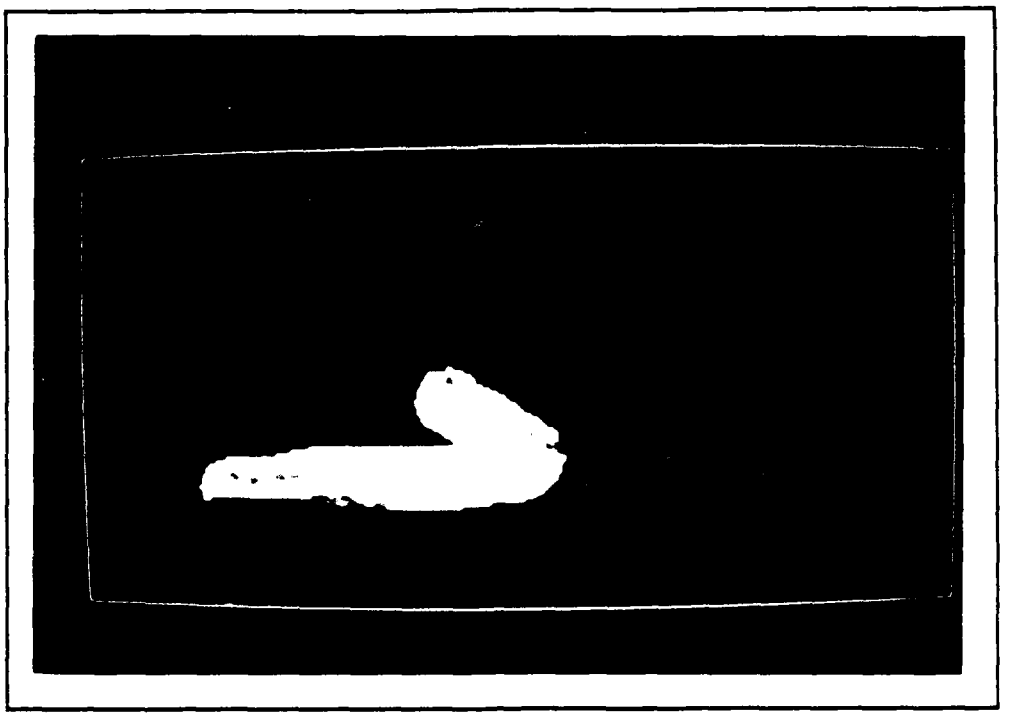

Figure 3.11 Region of interest (1F) overlayed on the filtered oblique ionogram. Goose Bay, Labrador to Millstone Hill, Massachusetts; April 5, 1988, 1908UT.

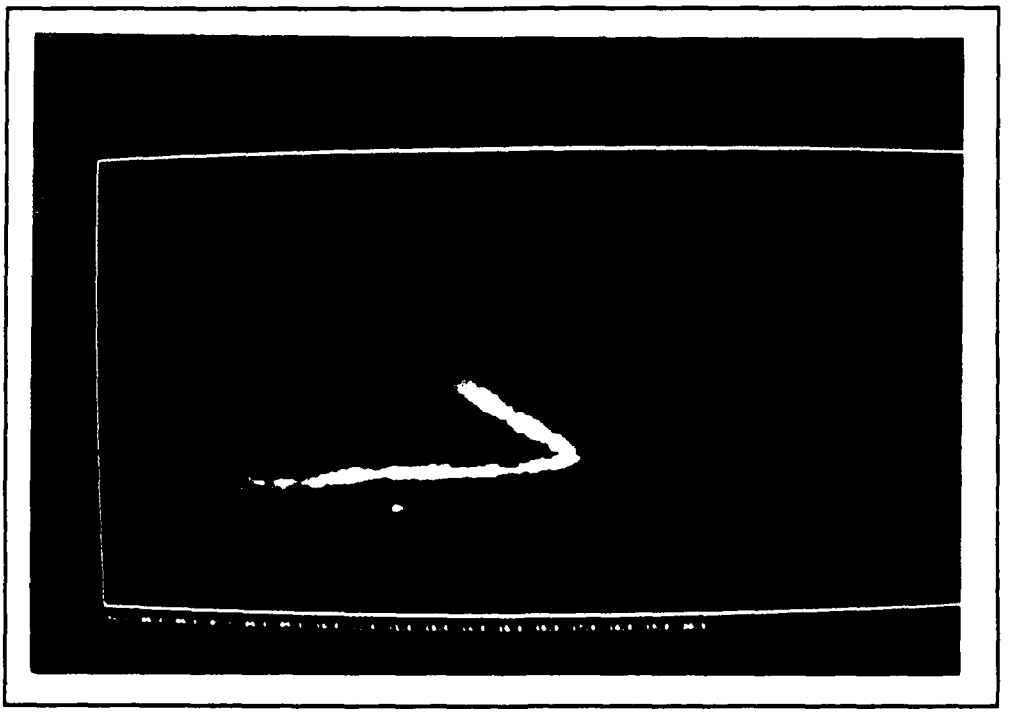

Figure 3.12 Resulting oblique 1F ionogram in the region of interest. Goose Bay, Labrador to Millstone Hill, Massachusetts; April 5, 1988, 1908UT.

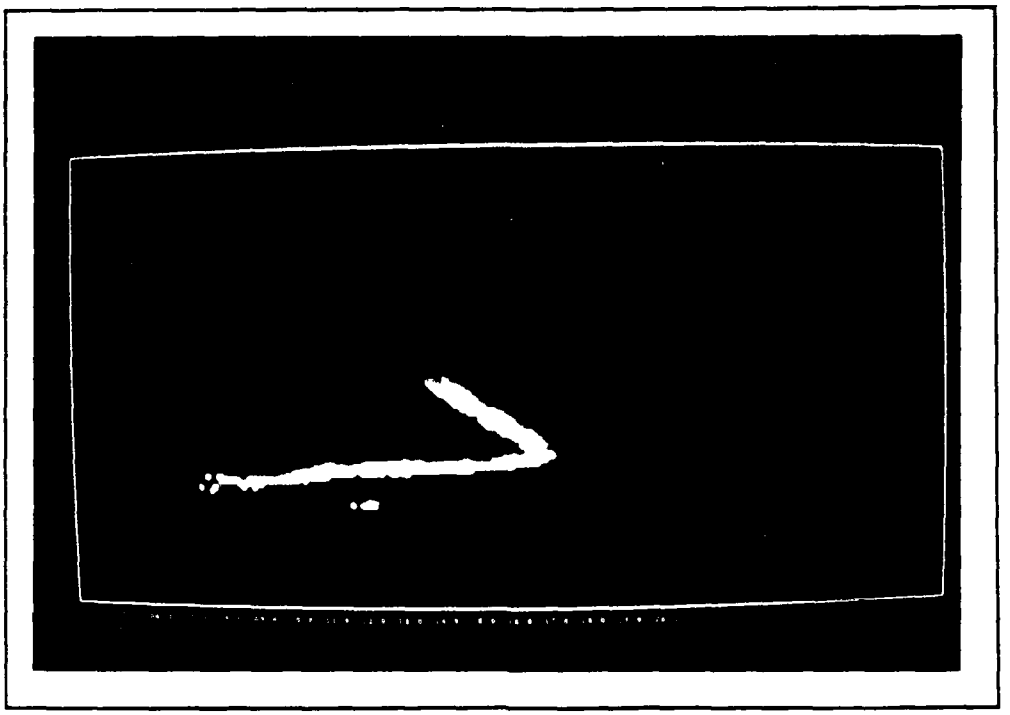

Figure 3.13 Scaled oblique 1F trace shown in white along with the 1F oblique ionogram. Goose Bay, Labrador to Millstone Hill, Massachusetts; April 5, 1988, 1908UT.

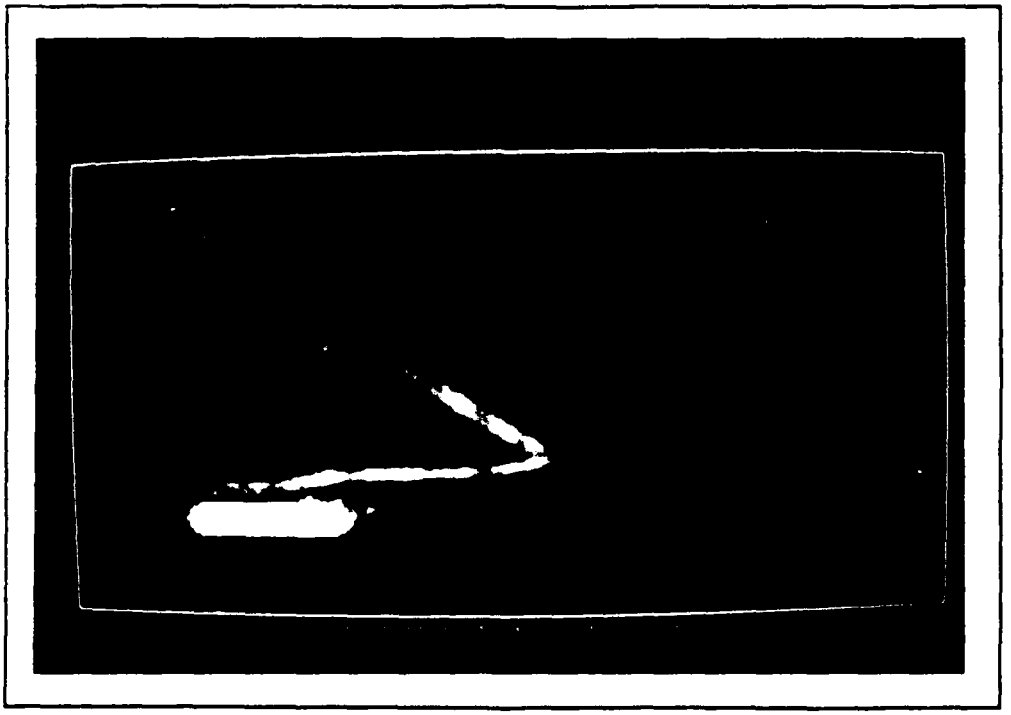

Figure 3.14 Region of interest (1E) overlayer on the filtered oblique ionogram. Goose Bay, Labrador to Millstone Hill, Massachusetts; April 5, 1988, 1908UT.

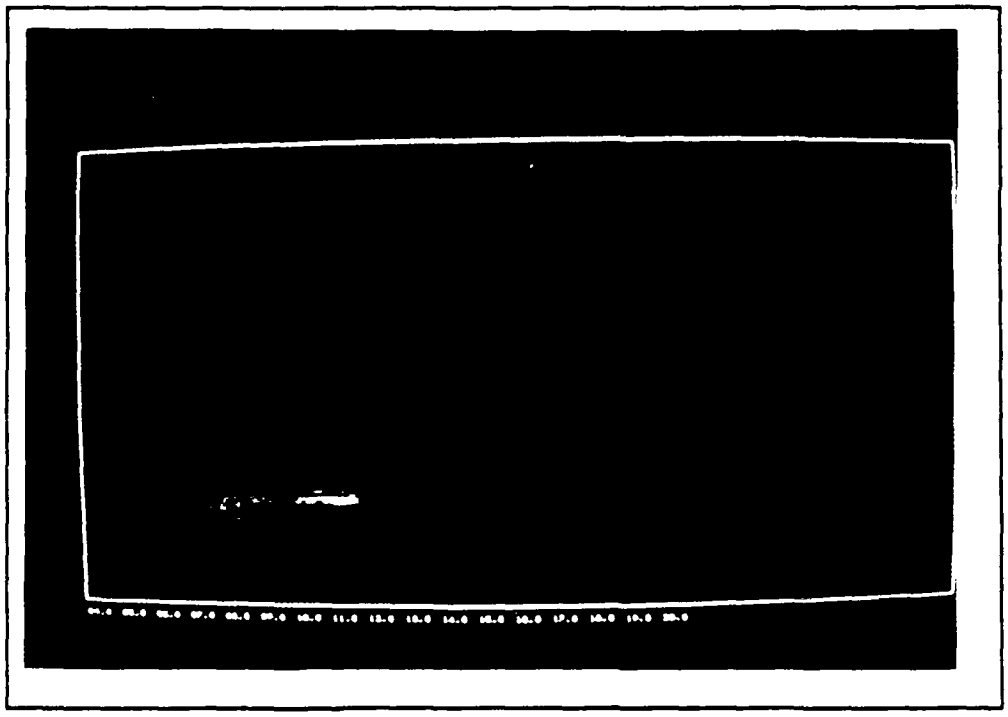

Figure 3.15 Resulting oblique 1E trace shown with the region of interest. Goose Bay, Labrador to Millstone Hill, Massachusetts; April 5, 1988, 1908UT.

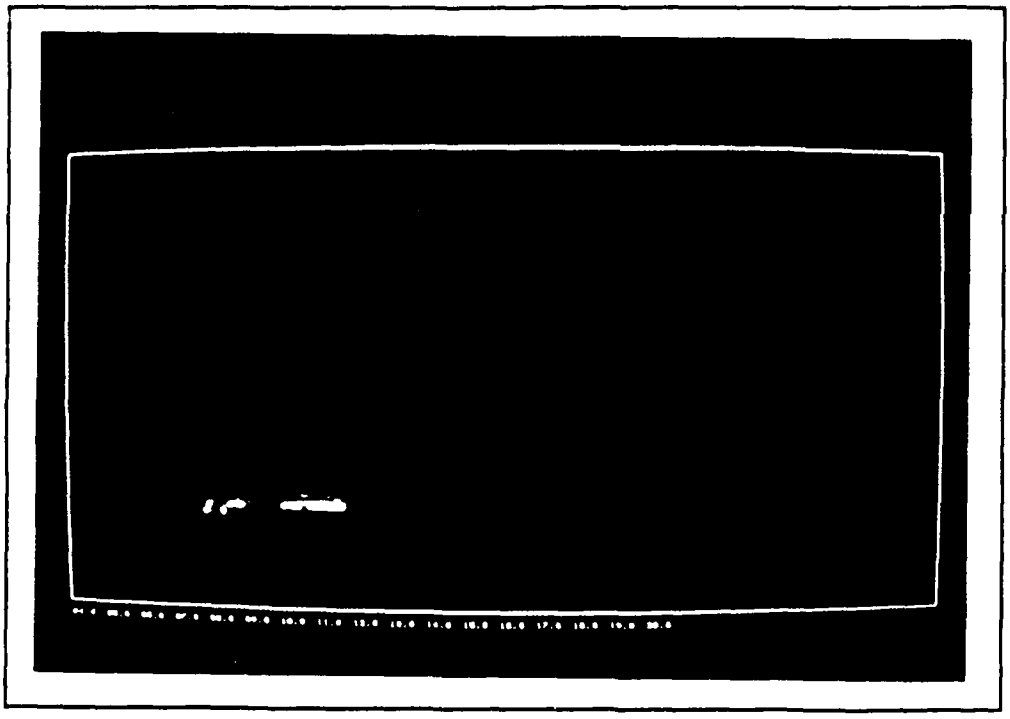

Figure 3.16 Scaled oblique 1E trace shown in white along with the 1E oblique ionogram. Goose Bay, Labrador to Millstone Hill, Massachusetts; April 5, 1988, 1908UT.

are identical to that used for the 2500 km data. The E trace region of interest is defined as all points within three range bins and/or sounding frequencies of the synthesized oblique E trace. Figure 3.11 shows the F trace region of interest overlaid on the filtered oblique ionogram data. Note that although the high angle ray portion of the one hop F oblique echo trace has the same slope as the corresponding portion of the region of interest, the actual data has an extended low frequency segment of the high angle ray that is excluded from further processing. Figure 3.12 shows the resulting oblique F echo trace, i.e. only that portion of the filtered oblique ionogram data in the region of interest. Figure 3.13 shows the resulting scaled oblique F trace in white along with the entire F oblique echo trace. Figure 3.14 shows the E trace region of interest overlaid on the filtered oblique ionogram data. Note, in this case a segment of the actual E echo trace, at sounding frequencies above the E region of interest, has already been incorrectly labeled as part of the F trace and is hence excluded from the E trace at this point. Figure 3.15 shows the resulting oblique E echo trace, i.e. only that portion of the filtered oblique ionogram data in the region of interest. Figure 3.16 shows the resulting scaled oblique E trace in white along with the entire E oblique echo trace.

4.0 OBLIQUE IONOGRAM SCALING ALGORITHM STATUS

The initial development of the vertical end point ionogram-based oblique scaling algorithm has been demonstrated. This algorithm requires a scaled vertical ionogram at one end of the oblique path to generate an initial estimate of the midpoint ionosphere that is used in the subsequent signal processing and pattern recognition stages of the algorithm. While this algorithm performs well for relatively short oblique paths, where a reasonable estimate of the midpoint ionosphere can be obtained from the scaled vertical ionogram, it performs in a less reliable manner for cases where the length of the oblique path makes it difficult to estimate the midpoint ionosphere from the endpoint data. However, the signal processing aspects of this algorithm, which produce estimates of the oblique echo traces from the raw oblique ionograms, can also be utilized in the proposed model-based oblique ionogram scaling algorithm. A data base of approximately 200 digital oblique ionograms has been recorded. These ionograms will also be used in the development and evaluation of the model-based oblique ionogram scaling algorithm. The development of the model-based oblique ionogram scaling algorithm, continued data collection and evaluation of the resulting oblique ionogram scaling algorithm for a wide range of data is in progress.